THE JOURNAL OF BIOLOGICAL CHEMISTRY VOL. 285, NO. 20, pp. 14871–14881, May 14, 2010

Identification and Characterization of Mitochondrial Targeting Sequence of Human Apurinic/Apyrimidinic Endonuclease 1*[S]

Received for publication, September 24, 2009, and in revised form, March 15, 2010 Published, JBC Papers in Press, March 15, 2010, DOI 10.1074/jbc.M109.069591

Mengxia Li[‡1], Zhaoyang Zhong[‡1], Jianwu Zhu[‡1], Debing Xiang[§], Nan Dai[‡], Xiaojing Cao[‡], Yi Qing[‡], Zhenzhou Yang[‡], Jiayin Xie[‡], Zengpeng Li[§], Laura Baugh[¶], Ge Wang[‡], and Dong Wang[‡2]

From the [‡]Cancer Center and [§]Department of Pathology of Research, Institute of Surgery, Daping Hospital, Third Military Medical University, Chongqing 400042, China and the [¶]Department of Biology, University of Dallas, Irving, Texas 75062

Dually targeted mitochondrial proteins usually possess an unconventional mitochondrial targeting sequence (MTS), which makes them difficult to predict by current bioinformatics approaches. Human apurinic/apyrimidinic endonuclease (APE1) plays a central role in the cellular response to oxidative stress. It is a dually targeted protein preferentially residing in the nucleus with conditional distribution in the mitochondria. However, the mitochondrial translocation mechanism of APE1 is not well characterized because it harbors an unconventional MTS that is difficult to predict by bioinformatics analysis. Two experimental approaches were combined in this study to identify the MTS of APE1. First, the interactions between the peptides from APE1 and the three purified translocase receptors of the outer mitochondrial membrane (Tom) were evaluated using a peptide array screen. Consequently, the intracellular distribution of green fluorescent protein-tagged, truncated, or mutated APE1 proteins was traced by tag detection. The results demonstrated that the only MTS of APE1 is harbored within residues 289–318 in the C terminus, which is normally masked by the intact N-terminal structure. As a dually targeted mitochondrial protein, APE1 possesses a special distribution pattern of different subcellular targeting signals, the identification of which sheds light on future prediction of MTSs.

Human APE1 (apurinic/apyrimidinic endonuclease) is an important multifunctional protein that plays a central role in the cellular response to oxidative stress. The two major activities of APE1 are DNA repair and redox regulation of transcriptional factors. On one hand, APE1 functions as a critical rate-limiting enzyme in DNA base excision repair and accounts for nearly all of the AP site incision activities in cell extracts (1). On the other hand, APE1 also exerts unique redox activity to regulate the DNA binding affinity of certain transcriptional factors by controlling the redox status of their DNA-binding domain (2). Inhibition of the redox function of APE1 blocks murine endothelial cell growth and angiogenesis and also blocks the growth of human tumor cell lines (3). The biological importance of APE1 is highlighted by the finding that APE1 knockout mice exhibit an embryonic lethal phenotype (4). Although APE1 has long been labeled as a nuclear protein, a growing body of evidence has shown that the subcellular distribution of APE1 can be cytoplasmic in some cell types with high metabolic or proliferative rates, with predominant localization in the mitochondria and the endoplasmic reticulum (5–7). Recent mitochondrial proteomic studies have further confirmed the existence of APE1 in the mitochondria (8). Considering the importance of the mitochondria in cellular response to oxidative stress, the roles of APE1 in the mitochondria have been extensively investigated. A number of studies have shown that the initial mitochondrial APE1 protein level is scarce (*i.e.* it is not easily detected by regular immunotechniques) (8, 9). When subjected to different stimuli of oxidative stress, such as hydrogen peroxide, the mitochondrial APE1 level is significantly increased in a dose- and time-dependent fashion (9, 10). Therefore, the mitochondrial targeting of APE1 seems to be conditional.

The mitochondrial DNA is a small circular genome, coding a mere 37 gene products, including 24 tRNAs and 13 proteins, in contrast to the more than 1000 proteins found in the mitochondrion (11). Hence, most mitochondrial proteins are encoded by the nuclear genome and translocated into the mitochondria. Like the proteins destined for other subcellular organelles, the mitochondrially targeted proteins possess targeting signals within their primary or secondary structure that direct them to the organelle with the assistance of elaborate protein translocating and folding machines (12, 13). The nucleus-encoded mitochondrially targeted preproteins are recognized by the receptors on the mitochondrial surface and are subsequently translocated across the outer mitochondrial membranes through a general import pore that assembles into a high molecular weight complex, termed the preprotein translocase of the outer mitochondrial membrane (Tom) (13, 14). The three Tom subunits, Tom20, Tom22, and Tom70, expose major portions on the cytosolic side of the outer membrane and function as import receptors for distinct classes of the preproteins *in vivo* and *in organello* (15). The purified cytosolic domains of these import receptors were validated to specifically bind the mitochondrial preproteins *in vitro* (16). Protein

* This work was supported by National Natural Science Foundation of China Grant 30670628 (to D. W.) and by the Natural Science Research Foundation of the Third Military Medical University (to Z. Z.).

[S] The on-line version of this article (available at http://www.jbc.org) contains supplemental Figs. S1 and S2.

[1] These authors contributed equally to this work.

[2] To whom correspondence should be addressed: Cancer Center, Research Institute of Surgery, Daping Hospital, Third Military Medical University, 10 Changjiang Zhi Rd., Daping Yuzhong District, Chongqing 400042, China. Tel./Fax: 86-23-68894062; E-mail: dongwang64@hotmail.com.

import studies with isolated mitochondria indicate that Tom20 and Tom22 function as a heterodimer receptors for the typical mitochondrial preproteins that carry the cleavable N-terminal mitochondrial targeting sequence (MTS).[3] This signal is classically characterized as an N-terminal motif predicted to form an amphipathic helix that is ~15–70 residues in length and enriched in positively charged basic residues (17). Tom70 is reported to be required for the import of non-cleavable preproteins that have been shown to have specificity for carrier proteins destined for the inner mitochondrial membrane (18).

It is obvious that mitochondrial localization is a prerequisite for the functions of APE1. APE1 is a 36-kDa molecule that cannot be translocated to the mitochondria through a passive transport process and so the mitochondrial targeting of APE1 involves an active mechanism. Hence, it is very important to identify the MTS of APE1. However, the mitochondrial translocation mechanism of APE1 is not well characterized because the bioinformatics analysis has failed to position the MTS (19). Previous efforts using computer-aided signal sequence-searching tools, including MitoProt and TargetP, have indicated that APE1 has a low score in MTS prediction. Instead, a classic nuclear localization signal (NLS) is identified and characterized at the N terminus of APE1 (20). In contrast with exclusively mitochondrially targeted proteins, APE1 is considered to be a dually targeted mitochondrial protein that is mainly destined for the nucleus. Dinur-Mills *et al.* (21) found that the dually targeted mitochondrial proteins have a weaker MTS and a lower whole protein net charge. The proteins containing these unconventional targeting signals will most probably escape prediction using a bioinformatics-based approach. Therefore, experimental approaches are usually used to identify and characterize the MTS of preproteins that are localized to the mitochondria.

This study focuses on the identification and characterization of the MTS of APE1 and further explores the possible import machinery that mediate APE1 translocation. Aiming to diminish the possible bias of both methods, we have employed a strategy combining two sophisticated approaches to identify and characterize the MTS of APE1, including biochemical and morphological approaches. The results demonstrate that the MTS of APE1 resides within residues 289–318 of the C terminus, which are normally masked by the intact N-terminal structure. This may be the explanation to its predominant nuclear localization and conditional mitochondrial targeting after oxidative stress. Moreover, as a dually targeted mitochondrial protein, APE1 possesses a special distribution pattern of different subcellular targeting signals, the discovery of which sheds light on the future identification of MTSs.

EXPERIMENTAL PROCEDURES

Materials—Dulbecco's modified Eagle's medium, fetal bovine serum, and transfection reagent Lipofectamine 2000 were purchased from Invitrogen. The eukaryotic expression vectors pEGFP-N2 and pEGFP-C1 were from Clontech (Mountain View, CA). H_2O_2, menadione, ampicillin, penicillin, streptomycin, proteinase K, RNase A, isopropyl-β-D-thiogalactopyranoside, imidazole, and polyvinylidene difluoride transfer membranes were from Sigma. High performance nickel-Sepharose was purchased from GE Healthcare. MitoTracker Red CMXRos, TO-PRO3 nuclear probe, and COX IV antibody were from Molecular Probes, Inc. (Eugene, OR). T4 ligase, restriction endonucleases, and high fidelity *Pfu* DNA polymerase were from Promega (Madison, WI). Protein interaction His tag pull-down kit, SuperSignal WestPico chemiluminescent reagents, horseradish peroxidase-conjugated His probe, and horseradish peroxidase-conjugated secondary antibodies were from Pierce. The monoclonal antibody against hAPE1 was from Novus Biological (Littleton, CO). The anti-Pax5, anti-GFP and fluorescein isothiocyanate-conjugated secondary antibody were purchased from Santa Cruz Biotechnology, Inc. (Santa Cruz, CA).

Cell Culture and Transfection—The human cervical cancer cell line HeLa was obtained from the American Type Culture Collection (Manassas, VA). The cells were maintained in high glucose Dulbecco's modified Eagle's medium supplemented with 10% (v/v) fetal bovine serum, 50 mg/ml penicillin/streptomycin, and 2 mM L-glutamine in 5% CO_2 at 37 °C and passaged 2–3 times/week. For transfection, 2000 cells were plated into one well of a 96-well plate and incubated under normal conditions overnight until they reached ~85% confluence. The different plasmids were then transfected into human umbilical vein endothelial cells using Lipofectamine 2000 transfection reagent according to the manufacturer's protocol.

Immunofluorescence and Confocal Laser-scanning Microscopy—HeLa cells were grown on a slide at a density of 2×10^4 cells/well in a 6-well plate for 24 h. Then the HeLa cells were treated with 100 μM H_2O_2 or menadione bisulfate or incubated in a hypoxia condition with 1% oxygen content for 6 h. The culture media were removed, and the cells were incubated with a culture medium containing 200 nM MitoTracker Red CMXRos probe for 30 min at 37 °C. After washing twice in cold PBS, the cells were fixed with 2% (w/v) paraformaldehyde in PBS at 4 °C for 20 min. Then the cells were permeabilized with 0.5% Triton X-100 in PBS for 15 min at room temperature. The slides were washed twice with PBS, and the cells were blocked with normal goat serum at 37 °C for 30 min, followed by immunobinding by APE1 antibody at a dilution of 1:200 for 2 h. Subsequently, the cells were incubated with fluorescein isothiocyanate-conjugated secondary antibody for 30 min at 37 °C. After washing, the cells were stained with TO-PRO3 nuclear probe at a dilution of 1:5000 for 5 min. Then the cells were mounted and visualized under a Leica confocal laser-scanning microscope (TCS SP5) available at the central laboratory of the Third Military Medical University. For multicolor fluorescence, the red, green, and blue signals were collected simultaneously and then superimposed.

Organelle-enriched Fractionation—The nuclear extracts from the treated and control groups were isolated as described previously (22). Ten million HeLa cells were collected and resuspended in 500 μl of hypotonic lysis buffer. After incubation for 10 min, the nuclei were collected by centrifugation at 500 $\times$ *g*, and the nuclear pellet was resuspended and incubated with 100

[3] The abbreviations used are: MTS, mitochondrial targeting sequence; GFP, green fluorescent protein; NLS, nuclear localization signal; PBS, phosphate-buffered saline; EGFP, enhanced GFP.

μl of buffer B (10 mM HEPES, 100 mM NaCl, 1.5 mM $MgCl_2$, 0.1 mM EDTA, 0.1 mM dithiothreitol, 5 mM phenylmethylsulfonyl fluoride, pH 7.9) for 20 min at 4 °C. After incubation, the samples were centrifuged at 10,000 × *g* at 4 °C for 20 min.

The cytosolic and mitochondrial crude fractions were prepared by differential centrifugation as described previously (22). Briefly, 5×10^8 cells were collected and resuspended in 1 ml of grinding medium and pulse-sonicated on ice at 30 watts for 15 s, ensuring 50–70% cell lysis. Then the lysate was centrifuged for 12 min at 800 × *g*, and the supernatant was immediately centrifuged for 20 min at 8500 × *g* at 4 °C. The obtained supernatant contained the cytosolic fraction. The mitochondrial pellet was resuspended with 100 μl of buffer S (150 mM sucrose, 40 mM KCl, 25 mM Tris-HCl, 1 mg/ml bovine serum albumin, pH 7.4) and sonicated on ice at 45 watts, three times for 15 s each, and then precipitated by centrifugation for 20 min at 10,000 × *g* at 4 °C.

Western Blots—Twenty micrograms of protein from nuclear, cytosolic, or mitochondrial fractions was applied to 12% SDS-polyacrylamide gels and electrophoresed to resolve proteins. The proteins were then transferred to polyvinylidene difluoride membranes and blocked in TBST containing 5% (w/v) nonfat dry milk. The membrane was incubated with mouse anti-hAPE1 primary antibody (1:2000), mouse anti-COX IV primary antibody (1:1000), and mouse anti-Pax5 primary antibody (1:1000) overnight at 4 °C. The membrane was then washed three times in TBST and incubated with horseradish peroxidase-labeled secondary antibody for 1 h at 37 °C. The membrane was reacted with chemiluminescent reagents and revealed with BioMax-Light films (Eastman Kodak Co.). The band intensities were analyzed using the Gel Doc 2000 apparatus and software (Quantity One, Bio-Rad).

Expression and Purification of Tom Proteins in Escherichia coli—The prokaryotic expression vectors carrying cytosolic domains of the three Tom proteins, named pET19b-yTom20cd-His10, pET19b-yTom22cd-His10, and pET19b-yTom70cd-His10 were gifts from Prof. Nikolaus Pfanner. The expression and purification were performed as described with modifications (15). Briefly, the *E. coli* strain BL21 (DE3) was transformed with three plasmids, and protein expression was induced by the addition of 0.1 mM isopropyl-β-D-thiogalactopyranoside for 4 h. The bacterial pellet was resuspended in 5 mM imidazole, 500 mM NaCl, and 20 mM Tris-HCl, pH 7.9, and then sonicated. After centrifugation, the supernatant was applied to columns containing nickel-Sepharose resin (GE Healthcare). After five washes with different concentrations of imidazole (20–200 mM), 500 mM NaCl, and 20 mM Tris-HCl, pH 7.9, the Tom proteins were eluted with 1 M imidazole, 500 mM NaCl, and 20 mM Tris-HCl, pH 7.9, and dialyzed against 1× PBS, pH 7.4. The purities of Tom proteins were analyzed using SDS-polyacrylamide gel electrophoresis, and the protein concentrations were measured using the Bradford assay. To evaluate the affinity of the purified Tom proteins to His probe, the Tom proteins were separated using SDS-PAGE and then subjected to Western blot against horseradish peroxidase-conjugated His probe (1:10,000).

Peptide Array Screen—The cellulose-bound peptide array was designed and prepared by automated spot synthesis (INTAVIS Bioanalytical Instruments AG, Köln, Germany). All of the incubations were processed in a chamber (NUNC™ 4-well slide processing dish; Thermo Fisher Scientific, Roskilde, Denmark). To analyze the Tom protein-binding activity, the array was first blocked in 1% nonfat milk, TBST (w/v) solution at 37 °C for 4 h. After washing three times with TBST, the array was incubated overnight with 150 nM purified Tom protein diluted in TBST at 4 °C with gentle shaking. The nonspecifically bound protein was removed by washing the array with TBST for 5 min at room temperature and then incubated with horseradish peroxidase-conjugated His probe (1:10,000) for 1 h at 37 °C. The Tom protein bound to the peptide array was detected using a chemiluminescent blotting substrate (ECL, Pierce). A quantitative measurement of the binding strength was performed with Spotfinder software (Dana-Farber Cancer Institute, Boston, MA), which included subtraction of the local background for each peptide spot. The means of at least three independent experiments for each peptide spot were used (average units) (23). The values for the different membranes were adjusted by the use of identical reference peptides on each membrane. The 24-residue-long MTS from manganese-superoxide dismutase was adopted as a positive control (sequence: MLSRAVCGTSRQLAPALGYLGSRQ) and diluted in multiproportions.

His Tag Pull-down Assay—The His tag pull-down assay was performed using the ProFound™ pull-down poly-His protein-protein interaction kit (Pierce) according to the protocol provided by the manufacturer. An immobilized cobalt chelate was added to the Handee™ spin columns and incubated with the purified Tom proteins for 4 h at room temperature to bind their His tag as bait proteins. Then the unbound Tom proteins were removed with the wash buffer. The HeLa cells were lysed by adding 1 ml of lysis buffer to each culture dish and incubated on ice for 30 min. The plates were scraped, and the cell lysate was placed in a centrifuge tube. The protein concentration of the cell lysate was analyzed using the Bradford assay. Then the cell lysate was added to a column containing the bound Tom proteins and incubated overnight at 4 °C with gentle shaking. After incubation, the suspensions were centrifuged at 7000 × *g* at 4 °C and washed three times with cold TBS. The supernatant was removed after the third wash. Then the protein-protein complex was eluted using the elution buffer and analyzed using 12% SDS-PAGE, followed by Western blotting using monoclonal antibodies for APE1 (Novus Biological).

Truncated and Mutated APE1 Expression Plasmid Construction—Different oligonucleotides were designed as primers to amplify the target truncated APE1 cDNA fragments by PCR from pcDNA3.1-APE1 vector containing the full-length APE1 cDNA sequence that was constructed in the previous work. For the vectors based on pEGFP-N2, all of the forward primers were added as initiation codons of the ATG and EcoRI sites, and all of the reverse primers were added to the BamHI site at their 5′-ends. For the vectors based on pEGFP-C1, all of the forward primers were added to the EcoRI site, and all of the reverse primers were added as termination codons of TGA and BamHI sites at their 5′-ends. PCR reactions were processed using high fidelity *Pfu* DNA polymerase according to the manufacturer's instruction. The resulting PCR products were subcloned into

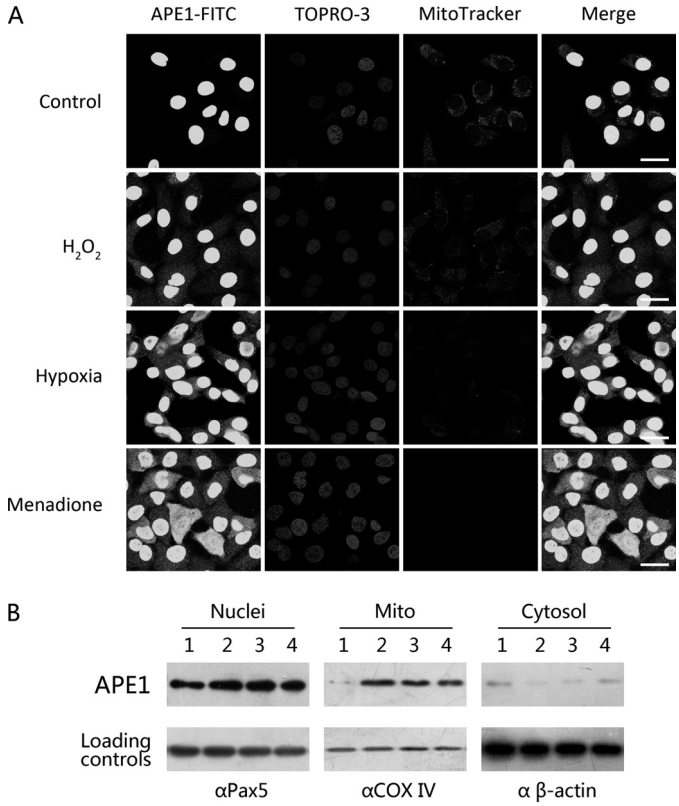

FIGURE 1. **Conditional mitochondrial targeting of APE1 after different stimuli.** HeLa cells were treated with 100 μM hydrogen peroxide or 100 μM menadione sodium bisulfate or cultured in hypoxic conditions (1% oxygen) for 6 h. The subcellular distribution of the APE1 protein was detected by immunofluorescence microscopy (*A*) and Western blot (*B*). Live cells were stained with Mito-Tracker Red mitochondrion-selective probe to visualize the mitochondria in the cells. The APE1 proteins were visualized by a standard immunofluorescence with fluorescein isothiocyanate-conjugated secondary antibody and are shown in *green*. The localization of APE1 in the mitochondria is displayed as *yellow-orange* by two superimposed staining patterns. *Scale bar*, 30 μm. Loading controls for the Western blot were Pax5 for the nucleus, COX IV for the mitochondria, and β-actin for the cytosol. *Numbers 1–4* represent control, hydrogen peroxide, menadione, and hypoxic pretreated groups, respectively.

pEGFP-N2 or pEGFP-C1 vectors. The fidelity of the constructed vectors was confirmed by sequencing (Sequencing and Synthesis Facility of Invitrogen (Shanghai, China)).

The mutated vectors were based on the constructed truncated APE1 plasmids, and the mutants were generated by QuikChange site-directed mutagenesis (Stratagene, La Jolla, CA) according to the manufacturer's protocol. All mutations were validated by sequencing.

RESULTS

APE1 Exhibits Dual Subcellular Targeting with the Nucleus as the Major Destination—To induce oxidative stress or DNA damage, the HeLa cells were treated with hydrogen peroxide and menadione sodium bisulfate or cultured in hypoxic conditions, as indicated under "Experimental Procedures." The subcellular localization of the APE1 protein was detected using immunofluorescence microscopy and Western blotting. The results in Fig. 1*A* show that APE1 was localized mainly in the nucleus of the untreated HeLa cells but was translocated to the cytoplasm and especially the mitochondria after hydrogen peroxide-, menadione-, or hypoxia-induced oxidative stress. The mitochondrial staining of APE1 was even stronger in menadione (the mitochondrial DNA-specific DNA damage-inducing agent)-treated HeLa cells. Additionally, a significant decrease in the mitochondrial membrane potential was observed after treatment with hydrogen peroxide, menadione, or hypoxic conditions. Although, the MitoTracker Red is not the typical mitochondrial membrane potential marker, it is hard to label the malfunctioning mitochondria when unfixed cells are labeled with MitoTracker Red. Actually, the loss of staining by the MitoTracker Red represented the abnormal mitochondrial function (24). To confirm the morphological findings, subcellular fractions of the nucleus, cytoplasm, and mitochondria from each group were subjected to Western blot. The results shown in Fig. 1*B* indicate that the major localization of APE1 in HeLa cells is the nucleus and that oxidative stress or menadione induced the translocation of APE1 to the mitochondria.

Recombinant Cytosolic Domains of Tom20, Tom22, and Tom70 Are Purified by Ni^{2+}-Nitrilotriacetic Acid Affinity Chromatography—To investigate the mitochondrion-targeting sequence of APE1, we first analyzed the binding property of the peptides derived from APE1 to the Tom receptors in a cell-free system. The results (supplemental Fig. S1) indicate that the expressions of all the Tom proteins were induced by 0.1 mM isopropyl-β-D-thiogalactopyranoside (supplemental Fig. S1*A*), and after 4 h of induction, the foreign proteins expressed ~10–20% of total cellular protein. To validate the purity of the Tom proteins that were isolated by Ni^{2+}-nitrilotriacetic acid chromatography, the 200 mM imidazole contained eluants separated by SDS-PAGE and then stained with Coomassie Brilliant Blue R250. The target proteins comprised >95% of the total eluants (supplemental Fig. S1*B*). Then 1 μg of the eluants was subjected to Western blot against the horseradish peroxidase-conjugated His probe. Supplemental Fig. S1*C* showed that only the target proteins that were shown as major bands in supplemental Fig. S1*B* were detected by the His probe, indicating that these contaminating bacterial proteins do not significantly impact the peptide array-based screen.

Tom20cd Preferentially Binds to Peptides Derived from APE1—Because the presequence of the mitochondrially targeted protein was recognized by the Tom proteins as a linear amino acid sequence, we designed a 15-mer peptide array for the Tom protein-binding site screen. Fifteen-amino acid peptides from APE1 that overlapped by 12 residues were covalently attached to the cellulose membrane. The MTS from the manganese-superoxide dismutase that has been extensively investigated as a classical N-terminal mitochondrial signal sequence was used as the positive control. The peptide consisting of the first 13 residues of APE1, which was validated to be an NLS, was chosen as the negative control. The films of the peptide arrays and their quantitative results are shown in Fig. 2. Tom20cd demonstrated the best binding efficacy among the three Tom proteins to the peptides derived from APE1 (Fig. 2*A*). Tom20cd was distributed in the regions of the first one-third of both the N terminus and C terminus. The binding affinity of Tom20cd to the C terminus of APE1 was generally higher than to the N terminus. The peak regions included peptides of residues 13–39, 49–63, 64–93, 211–240, 238–258, 265–279, and 289–312. However, when compared with Tom20cd, significant dif-

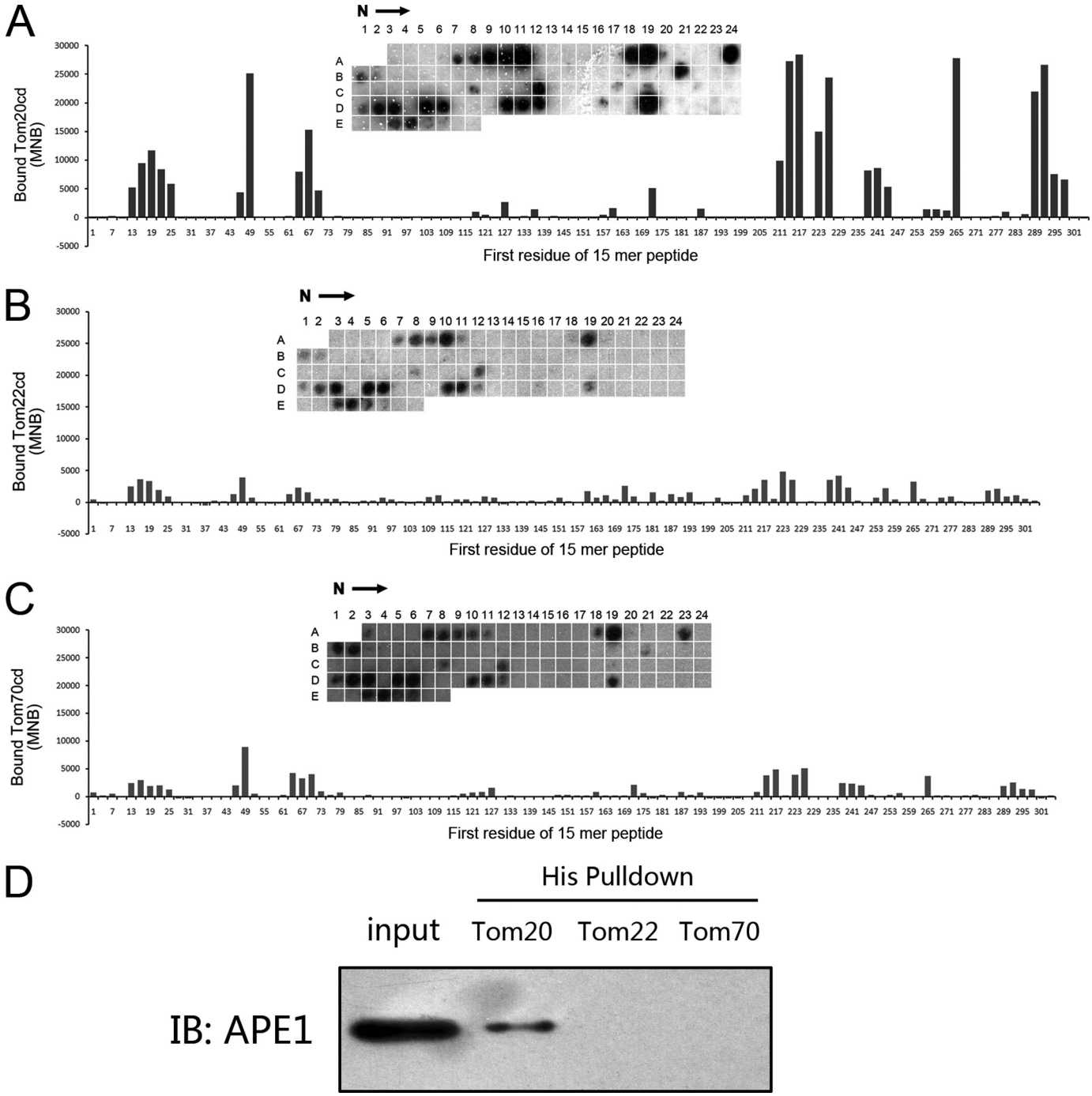

FIGURE 2. **Binding of the cytosolic domain of Tom20, Tom22, and Tom70 to a peptide array derived from APE1.** Binding of 150 nM Tom20cd (*A*), Tom22cd (*B*), and Tom70cd (*C*) to a peptide array consisting of 15 residues derived from APE1. The first peptide comprises amino acids 1–15 of APE1, the second peptide comprises residues 4–18, the third peptide comprises residues 7–21, and so on. The labeling originated from the peptide array. A quantitative measure of the binding strength was performed with Spotfinder software, which included subtraction of the local background for each peptide spot. The values for different membranes were adjusted by the use of identical reference peptides on each membrane. Results were obtained from three independent experiments. Tom proteins were immobilized by cobalt chelate and then incubated with HeLa cell extracts (*D*). The eluants from each Tom protein His tag pull-down experiment were separated using SDS-PAGE and then subjected to anti-APE1 antibody using Western blot (*IB*). The complete cellular extraction of the HeLa cell was also added as an input. As shown in Fig. 4, only Tom20cd interacted with APE1 from the HeLa cell extraction.

ferences were observed in the peptide scans of Tom22cd and Tom70cd binding. The APE1 peptide scan revealed that several binding sequences for Tom22cd were scattered over various regions of the whole protein (Fig. 2*B*), whereas the Tom70cd binding sequences were mainly located in both termini (Fig. 2*C*). Although the binding patterns of Tom20cd, Tom22cd, and Tom70cd were strikingly similar, the overall intensities of the interactions with Tom22cd and Tom70cd were significantly lower.

To determine which Tom protein is the most important to APE1 mitochondrial targeting, we performed the His tag pull-down assay to validate the interactions between the purified

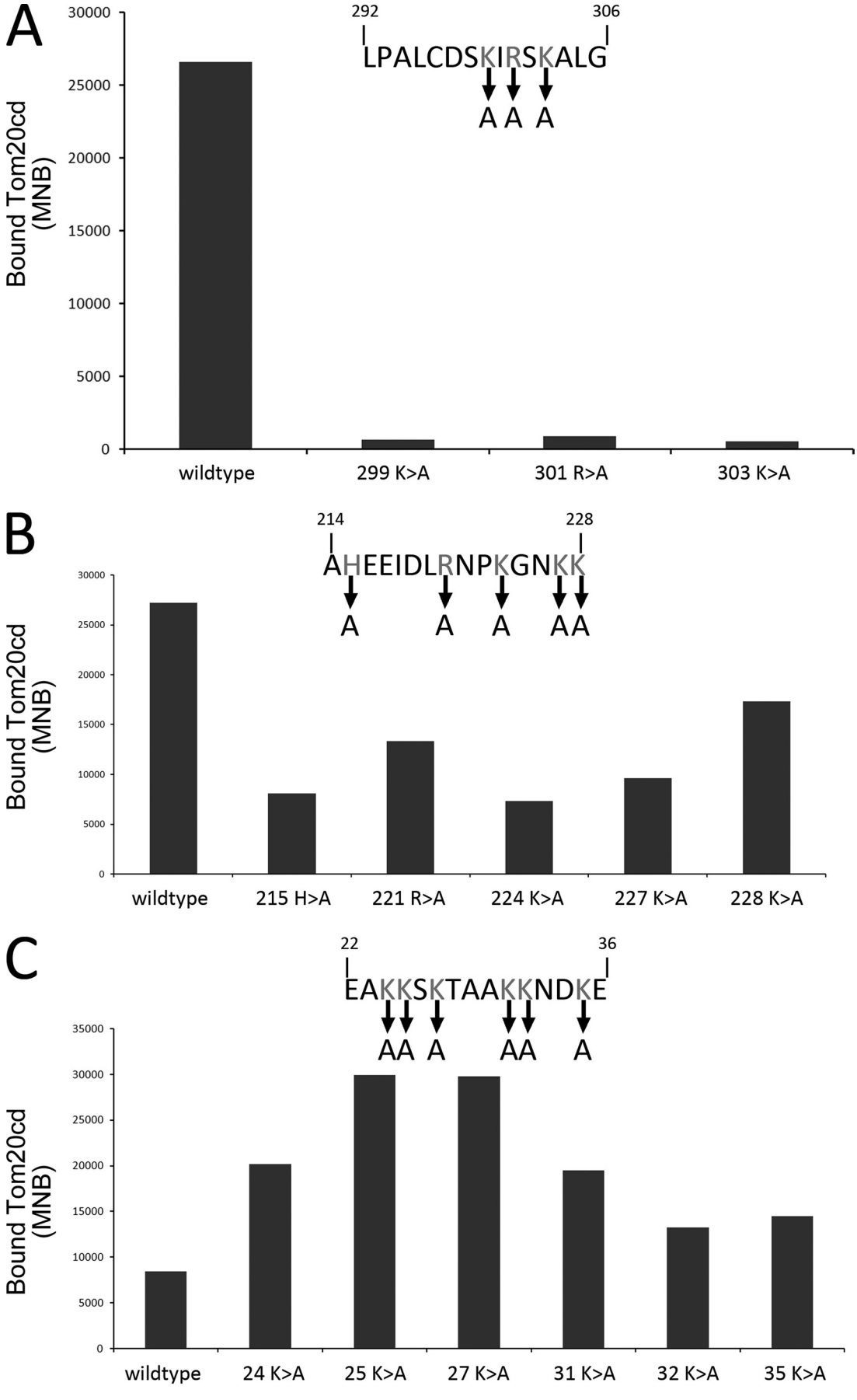
A
292
306
LPALCDSKIRSKALG
A A A
Bound Tom20cd (MNB)
30000
25000
20000
15000
10000
5000
0
wildtype
299 K>A
301 R>A
303 K>A
B
214
228
AHEEIDLRNPKGNKK
A A A AA
Bound Tom20cd (MNB)
wildtype
215 H>A
221 R>A
224 K>A
227 K>A
228 K>A
C
22
36
EAKKSKTAAKKNDKE
AA A AA A
Bound Tom20cd (MNB)
35000
30000
25000
20000
15000
10000
5000
0
wildtype
24 K>A
25 K>A
27 K>A
31 K>A
32 K>A
35 K>A

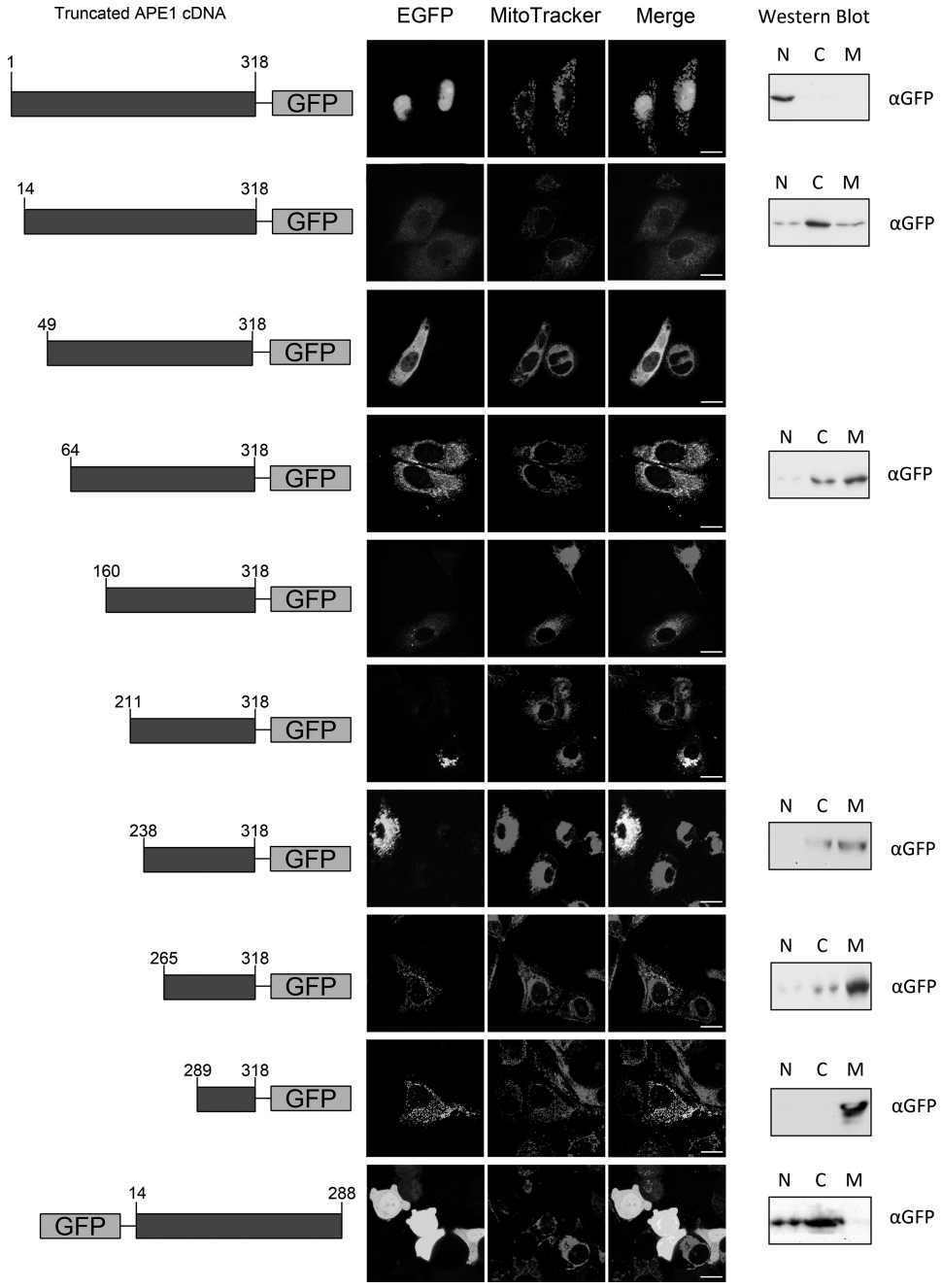

FIGURE 4. **Mapping of the APE1 domains responsible for mitochondrial targeting.** Immunofluorescent images depict the subcellular localization of different, truncated APE1 proteins in the HeLa cells at 48 h after transfection. Shown is a schematic representation of the N-terminal truncated mutants of APE1. GFP-fused positions are also indicated. *Scale bar*, 15 μm. The Western blots against GFP antibody in nuclear (*N*), cytosolic (*C*), and mitochondrial (*M*) enriched fractions of some groups are also shown on the *right*. The bands represent distribution of the exogenously expressed truncated APE1 proteins in each subcellular organelle.

Tom proteins and the cellular APE1 protein *in vitro*. Because the His tag was added at the terminus of the purified Tom proteins, these proteins together with their interactive proteins can be captured by the immobilized cobalt chelate. The eluants from each Tom protein pull-down experiment with an input of the whole cell lysate were separated using SDS-PAGE and then subjected to an anti-APE1 antibody using Western blot. The results shown in Fig. 2*D* indicate that only Tom20cd interacted with the full-length APE1 protein, which further confirms the findings of the peptide array. The results provided by the peptide screen assay together with the pull-down assay demonstrate that APE1 possesses higher affinity to Tom20 than to Tom22 or Tom70, which led to the hypothesis that mitochondrial translocation of APE1 may be through a Tom20-dependent pathway.

Alanine Replacement of Three Positively Charged Amino Acids at the C terminus of APE1 Diminished Affinity to Tom20cd—We further analyzed the amino acid composition of the "hot spot" peptides with higher affinities to Tom20cd. Interestingly, most of these regions are rich in positively charged amino acids, including lysine, arginine, and histidine. Thus, the regions containing tandems of positively charged residues, including residues 22–36, 214–228, and 292–306, were picked. To investigate the impact of these charged residues on the binding efficacy to Tom20cd, we subsequently designed another peptide array using the "alanine walk" method, which replaced each target amino acid position with alanine individually. The intensity of the interaction between the mutated peptides and Tom20cd was analyzed by the previously mentioned method. As shown in Fig. 3*C*, the wild type peptides of residues 292–306 (Fig. 3*A*) possessed robust affinity to Tom20cd, but the alanine replacement of Lys^{299}, Arg^{301}, and Lys^{303} diminished the binding efficacy of residues 292–306 to Tom20cd, which demonstrates that these residues may play significant roles in Tom20cd-APE1 interaction. Meanwhile,

FIGURE 3. **Screen critical residues for APE1 binding efficacy to Tom20cd by peptide array.** The peptides, containing tandems of positively charged amino acids including residues 292–306 (*A*), 214–228 (*B*), and 22–36 (*C*) were mutated using the "alanine walk" method, which replaced each target amino acid position individually with alanine (*A*). All of the wild type and mutated peptides were incubated with Tom20cd, and the binding intensity was measured and quantified using the aforesaid method. The binding efficacy of each wild type and its mutated form is shown in a *histogram*. The results are the average value of three independent experiments.

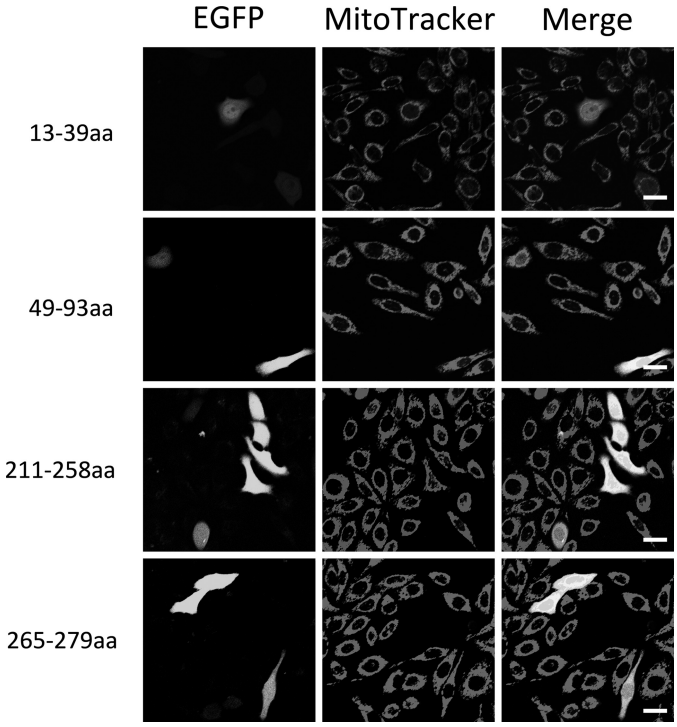

FIGURE 5. **Subcellular targeting of truncated APE1 protein of residues 113–139, 49–93, 211–258, and 265–279.** The other potential Tom20cd binding regions of APE1 were also tested for their mitochondrial targeting efficiency. Immunofluorescent images depict the subcellular localization of different, truncated APE1 proteins in the HeLa cells at 48 h after transfection. Mitochondria were visualized by MitoTacker Red probe. *Scale bar*, 30 μm. *aa*, amino acids.

mutations in peptide 214–228 (Fig. 3*B*) just slightly reduced the affinities to Tom20cd. Surprisingly, the alanine mutation at residues Lys^{24}, Lys^{25}, Lys^{27}, and Lys^{31} even enhanced the peptide binding efficacy to Tom20cd (Fig. 3*C*).

The Mitochondrial Targeting Sequence Localized at the C-terminal of APE1—Based on previous findings, truncated APE1 cDNA sequences were generated by the stepwise deletion of the "hot regions" that were found in the peptide screen by using PCR splicing and then subcloning in GFP-tagged eukaryotic expression vectors. The GFP was fused to the C terminus of the truncated APE1 proteins, and their subcellular distribution was visualized by laser confocal microscopy. The subcellular distribution of p53 and transcription factor A mitochondria was tested as nuclear and mitochondrial targeting controls to confirm the validity of our observation system. As shown in supplemental Fig. S2, at 48 h post-transfection, p53 was mainly targeted to the nucleus, whereas transcription factor A mitochondria mainly targeted to the mitochondria, indicating that the transfection and detection systems used in this experiment worked appropriately. We first fused the GFP tag to the C terminus of the truncated APE1, considering the functional importance of the N terminus of APE1 (Fig. 4). The full-length APE1 was mainly targeted to the nucleus in accordance with previous findings. However, when the first 13 residues of the N terminus, which was reported to harbor the major NLS of APE1, were deleted, the subcellular distribution shifted to a cytoplasmic dominant pattern. The truncated APE1, with the deletion of the N-terminal hot regions, including residues 14–318 and 49–318, was mainly located in the cytoplasm rather than in the mitochondria. There was no significant nuclear localization observed, which further confirmed that the NLS of APE1 is located in the first 13 residues of the N terminus. However, the truncated APE1 proteins containing only some C-terminal hot regions, including residues 211–318, 238–318, 265–318, and 289–318, were mainly targeted to the mitochondria complete overlapping of the MitoTracker staining. To exclude the possibility that there were internal targeting signals for other subcellular organs in the middle of the APE1 protein sequence, we deleted both residues 1–13 and 289–318, which are the nuclear and mitochondrial targeting signals, and transfected it into the HeLa cells. The truncated APE1 protein was diffusely distributed through the whole cell with no subcellular organelle-specific targeting observed. This distribution pattern, which is similar to the pattern of the pEGFP-N2 vector alone, was previously reported as a loss-of-signal targeting pattern representing the subcellular location of proteins that lack targeting signal sequences. Morphological observations were further confirmed by a subcellular organelle-enriched Western blot. The results of some of the critical truncated APE1 mutants are shown (Fig. 4). These results indicated that the MTS of APE1 resides in the C terminus appears masked by the N-terminal sequences that block the interaction between the C-terminal MTS of APE1 and the cytosolic subunits of the Tom protein.

To exclude the possibility that there are other MTSs that interfered with the C-terminal sequence of APE1, we further tested all of the possible regions according to the peptide array results. C-terminal EGFP-tagged truncated protein expression vectors carrying the residues 13–39, 49–93, 211–258 and 265–279 of APE1 were constructed and transfected into HeLa cells. The subcellular distribution of these proteins was observed by laser confocal microscopy and confirmed by Western blot. The results shown in Fig. 5 indicated these regions of APE1 have no specific mitochondrial targeting whereas only residues 13–39 may have a weak nuclear targeting signal and a preferential nuclear distribution.

Two Positively Charged Residues, Lys^{299} and Arg^{301}, in the C Terminus of APE1 Play Critical Roles in Its Mitochondrial Targeting—To determine which residues are critical to the mitochondrial targeting of the APE1 protein, we replaced three positively charged residues in the C terminus of APE1 with alanine using site-directed mutagenesis generating K299A, R301A, and K303A. These point-mutated vectors are based on the 289–318 truncated APE1 expression vectors with C-terminus-tagged EGFP. As shown in Fig. 6, K299A and R301A were distributed throughout the cell without obvious subcellular organelle-enriched locations, whereas the wild type sequence of 289–318 appears as a mitochondrial-specific distribution. Interestingly, we noticed that K303A appeared as two distribution patterns that were displayed in the same visual field in Fig. 6 (*third panel*). Most of the cells expressing K303A showed mitochondrially targeted distribution; however, some of these truncated mutants were observed in the cytoplasm or nuclei, indicating that K303A had a weak effect on its mitochondrial targeting. The K299A/R301A double mutated truncated APE1 protein showed a diffuse pattern, which further confirmed the

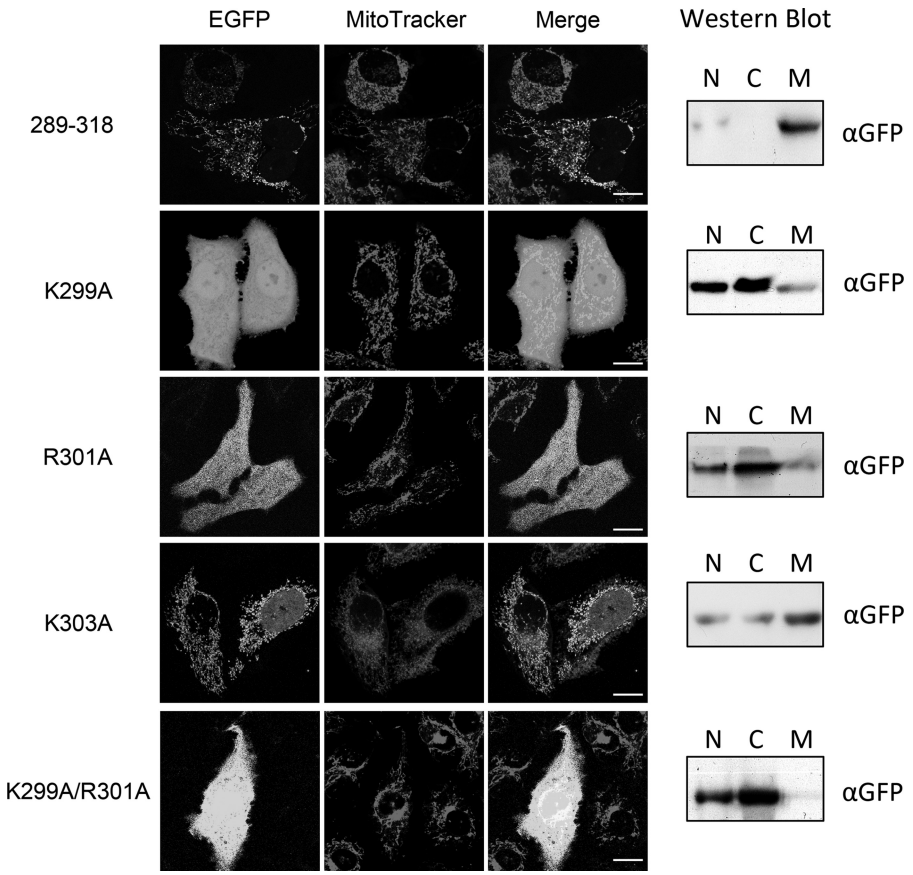

FIGURE 6. **Subcellular targeting of K299A, R301A, K303A, or K299A/R301A mutated APE1 observed by laser confocal microscopy.** K299A, R301A, K303A, or K299A/R301A mutated APE1 vectors are based on the 289–318 truncated APE1 expression vectors with C-terminally tagged EGFP. Subcellular localization of different truncated APE1 proteins in HeLa cells was observed by laser confocal microscopy at 48 h after transfection. *Scale bar*, 10 μm. The Western blot against GFP antibody in nuclear (*N*), cytosolic (*C*), and mitochondrial (*M*) enriched fractions are also shown on the *right*. The bands represent distribution of the exogenously expressed mutant in each subcellular organelle.

importance of Lys^{299} and Arg^{301} to the mitochondrial localization of APE1. These results further demonstrated that residues 289–318 were sufficient for mitochondrial targeting, and Lys^{299} and Arg^{301} were critical to the mitochondrial targeting of APE1.

Mutation of K299A and R301A Diminished Mitochondrial Translocation of APE1—We then tested the menadione-induced APE1 mitochondrial translocation affected by mutation of the two key residues Lys^{299} and Arg^{301}. The protein mitochondrial translocation of both wild type APE1 and full-length APE1 with the K299A/R301A mutations were compared. Using EGFP, we can easily track the translocation after menadione pretreatment. Due to the existence of the NLS of APE1, both wild type and the K299A/R301A full-length APE1 mutant mainly accumulate in the nucleus in untreated cells. However, when challenged with menadione, appreciable fractions of wild type APE1 relocalized to the mitochondria, whereas the majority of the mutant protein was in the nucleus. The nuclear and mitochondrial levels of exogenously expressed APE1 were confirmed by Western blot using anti-GFP antibody (Fig. 7).

DISCUSSION

APE1 was discovered as a dually targeted protein that is mainly distributed in the nucleus and conditionally targeted to the mitochondria. However, the mitochondrial targeting mechanism of APE1 has not been well elucidated. In our present study, we detect a unique MTS of APE1 by analyzing peptide affinities to Tom proteins and the subcellular targeting of truncated APE1 constructs. Our results indicate that the conditional mitochondrial targeting of APE1 depends on the C-terminal sequence of residues 289–318. We further demonstrated that Lys^{299} and Arg^{301} are the critical sites, and mutation of both sites abolishes APE1 mitochondrial translocation after menadione-induced oxidative stress.

We first employed peptide array to scan for a possible MTS by comparing the affinities to the Tom proteins. The results showed that the peptides with robust binding to Tom are scattered throughout the entire protein, making it difficult to determine the actual MTS of APE1. However, the results just highlighted some possible signal sequences for the future truncated assay. Surprisingly, the general patterns of binding for the different Tom proteins are strikingly similar. Regarding the different specificities of the three receptors, they have different affinities with the typical mitochondrial targeted proteins. However, there are some overlaps of affinities among these Tom proteins when interacting with purified peptides (16). One possibility is that APE1 is not a typical exclusive mitochondrial protein, and the MTS is not typical of a singly targeted mitochondrial protein. We believe the MTS of these proteins with multiple subcellular distributions can only be partially positioned by a peptide affinity assay. The mutant peptide assay also provided some potential critical residues for binding. The most noteworthy sites are Lys^{299}, Arg^{301}, and Lys^{303}, insofar as their replacement with alanine diminished the affinities of peptide to Tom20. Interestingly, the replacement of residues Lys^{24}, Lys^{25}, Lys^{27}, and Lys^{31} enhanced the affinities to Tom20. Because they are located in the N terminus of APE1, it is possible that these particular lysine residues function as suppressors to prevent the distribution of APE1 to the mitochondrion.

We then tested these possible targeting sequences by observing the subcellular distribution of the truncated forms of APE1. We noticed that when we deleted a small region of the N terminus, the truncated APE1 proteins were located in the cytoplasm. The truncated APE1 proteins containing residues 289–318 were specifically targeted to the mitochondria. Although all of the truncated proteins contained the MTS at their C terminus, the MTS could

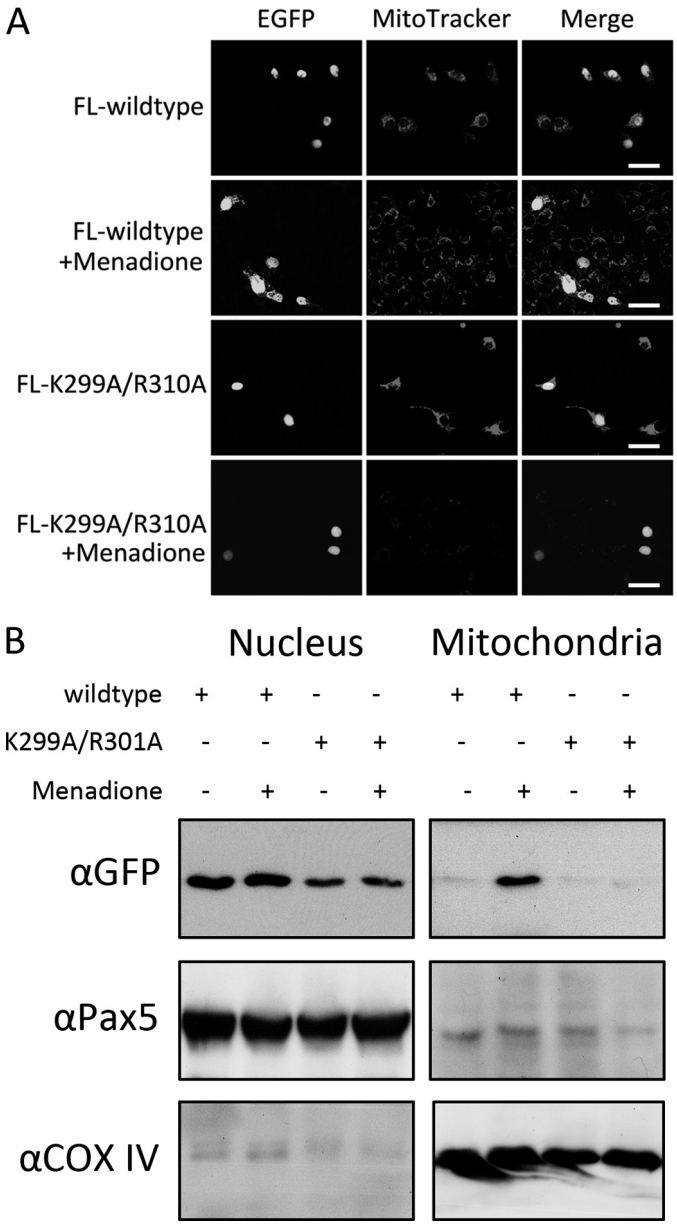

FIGURE 7. **Mitochondrial translocation of K299A/301R APE1 full-length mutant after menadione induction.** The K299A/R301A mutated APE1 full-length expression vector was transfected into HeLa cells at 48 h before 100 μM menadione treatment. EGFP visualized cellular images (*A*) and organelle-enriched Western blots (*B*) were obtained at 6 h after menadione treatment. The wild type APE1 protein expression vector was simultaneously treated as a control. *Scale bar*, 50 μm. The Western blot against GFP antibody in nuclear and mitochondrially enriched fractions of some groups are shown to depict the distribution of the exogenously expressed mutant in each organelle. The anti-Pax5 and COX IV Western blot were included to measure the cross-contamination between nuclei and mitochondria.

be located in the core of the APE1 protein, making it difficult for the MTS to be exposed to the Tom protein on the mitochondrial surface. We also tested possible mitochondrial targeting signals besides the MTS in the C terminus, based on the results of the peptide array. These results indicated that APE1 possesses a unique but weak MTS that is located in the C terminus and normally masked by the N terminus.

A previous study showed that isolated mitochondrial APE1 protein isolated from bovine liver is an N-terminally truncated form with the deletion of its NLS (8). It is noteworthy that the MTSs of most cleavable mitochondrial preproteins are cleaved by mitochondrial processing peptidase in the matrix. The mature form of the preproteins following processing is the major form in the mitochondrial matrix (25). According to this theory, the deleted residues of the truncated APE1 should harbor the MTS that is in its N terminus. However, based on the evidence provided by our present study, it is believed that the first 33 residues of the N terminus only harbor a classical NLS instead of both targeting signals. A plausible explanation is that the MTS of APE1 is overwhelmed by its NLS in the intact structure of the APE1 protein. APE1 conditionally targets the mitochondria only when its NLS is nonfunctional or deleted. One may ask why APE1 is targeted to the mitochondria after oxidative stress. Current studies are insufficient to address this question. A possible reason is that the intracellular redox imbalance alters the intact N-terminal conformation of APE1, which is the main domain exerting the redox function (26) and exposes the MTS to the Tom proteins in the mitochondrial outer membrane. Interestingly, the previous study has demonstrated that the NLS of Apn1, the APE1 homologue in yeast, resides in its C terminus, whereas its N terminus harbors a putative MTS. Pir1, an *O*-glycosylated protein required for yeast cell wall stability, was found to mask the NLS of Apn1 and also plays an active role in the mitochondrial targeting of the protein. Thus, the predicted N-terminal MTS of Apn1 is not sufficient for mitochondrial targeting in the absence of Pir1 (27). Because we could not get an accurate crystal structure of the C terminus of APE1, we then hypothesized that another possible mechanism of APE1 conditional mitochondrial targeting could be that the putative MTS of APE1 needs assistance to conduct the protein into the mitochondria by some protein chaperones that are induced by oxidative stress.

Our study further explored the possible mechanism of APE1 translocation to the mitochondria. The receptor Tom proteins, including Tom20, Tom22, and Tom70, mediate the preprotein transport in two major pathways. We found that APE1 was mainly recognized by Tom20cd, indicating that APE1 translocates to the mitochondria, possibly through a Tom20-dependent pathway. Tom20 recognizes a type of cleavable preproteins that possess a classical N-terminal MTS by binding via the hydrophobic portion of the signal sequence amphipathic helix. However, the identified MTS of APE1 in the present study is located in the C terminus, which is more similar to tail-anchored preproteins. The mitochondrial tail-anchored preproteins, including Bcl-2 and Tom20, were inserted into the mitochondrial outer membranes via a C-terminal transmembrane domain (28, 29). Although the exact localization of APE1 in the mitochondria has not been well characterized, according to its function in mitochondrial DNA repair, its distribution should accompany the mitochondrial DNA in the mitochondrial matrix. Thus, we are inclined to consider that the MTS of APE1 is not a tail-anchored signal but a special C-terminal mitochondrial signal that conducts it to the matrix of the mitochondria rather than to the outer membrane. Future studies to investigate APE1 location using submitochondrial fractions will help elucidate its mitochondrion-targeting mechanism.

In summary, to our knowledge, this is the first study that identifies and characterizes the MTS of APE1 and explores the mitochondrion-targeting mechanism of APE1. Our data support the finding that the MTS of APE1 is harbored in the last 30 residues of the C terminus of the protein, and Lys^{299} and Arg^{301} are critical to the oxidative stress-induced mitochondrial targeting of APE1. Our present study has also shown that APE1 translocates into the mitochondria mainly through the Tom20-dependent pathway, but detailed mechanisms remain to be elucidated. Moreover, this research sheds light on the possibility of a targeted therapeutic strategy using peptides that block the binding of the APE1 MTS to Tom receptors or dominant negative mutation of critical sites in the APE1 MTS with the aim of promoting apoptosis after oxidative stress.

Acknowledgments—We thank Dr. Nikolaus Pfanner and Dr. Jan Brix for providing the Tom protein expression vectors; Dr. Shangcheng Xu for help with the transcription factor A mitochondria and p53 vectors; Dr. Benjamin P. C. Chen, Dr. David J. Chen, Dr. Bruce Demple, and Dr. Hung Fung for critical comments on the manuscript; and Wei Sun, Liting Wang, Dr. Kai Fan, Dr. Zhiyong Liu, Dr. Zengtao Zhang, and Linli Zeng for excellent technical assistance.

REFERENCES

1. Chen, D. S., Herman, T., and Demple, B. (1991) *Nucleic Acids Res.* **19,** 5907–5914
2. Evans, A. R., Limp-Foster, M., and Kelley, M. R. (2000) *Mutat. Res.* **461,** 83–108
3. Luo, M., Delaplane, S., Jiang, A., Reed, A., He, Y., Fishel, M., Nyland, R. L., 2nd, Borch, R. F., Qiao, X., Georgiadis, M. M., and Kelley, M. R. (2008) *Antioxid. Redox Signal.* **10,** 1853–1867
4. Xanthoudakis, S., Smeyne, R. J., Wallace, J. D., and Curran, T. (1996) *Proc. Natl. Acad. Sci. U.S.A.* **93,** 8919–8923
5. Tell, G., Damante, G., Caldwell, D., and Kelley, M. R. (2005) *Antioxid. Redox Signal.* **7,** 367–384
6. Tomkinson, A. E., Bonk, R. T., and Linn, S. (1988) *J. Biol. Chem.* **263,** 12532–12537
7. Tell, G., Crivellato, E., Pines, A., Paron, I., Pucillo, C., Manzini, G., Bandiera, A., Kelley, M. R., Di Loreto, C., and Damante, G. (2001) *Mutat. Res.* **485,** 143–152
8. Chattopadhyay, R., Wiederhold, L., Szczesny, B., Boldogh, I., Hazra, T. K., Izumi, T., and Mitra, S. (2006) *Nucleic Acids Res.* **34,** 2067–2076
9. Mitra, S., Izumi, T., Boldogh, I., Bhakat, K. K., Chattopadhyay, R., and Szczesny, B. (2007) *DNA Repair* **6,** 461–469
10. Frossi, B., Tell, G., Spessotto, P., Colombatti, A., Vitale, G., and Pucillo, C. (2002) *J. Cell. Physiol.* **193,** 180–186
11. Asin-Cayuela, J., and Gustafsson, C. M. (2007) *Trends Biochem. Sci.* **32,** 111–117
12. Karniely, S., and Pines, O. (2005) *EMBO Rep.* **6,** 420–425
13. Becker, L., Bannwarth, M., Meisinger, C., Hill, K., Model, K., Krimmer, T., Casadio, R., Truscott, K. N., Schulz, G. E., Pfanner, N., and Wagner, R. (2005) *J. Mol. Biol.* **353,** 1011–1020
14. Dekker, P. J., Ryan, M. T., Brix, J., Müller, H., Hönlinger, A., and Pfanner, N. (1998) *Mol. Cell. Biol.* **18,** 6515–6524
15. Brix, J., Dietmeier, K., and Pfanner, N. (1997) *J. Biol. Chem.* **272,** 20730–20735
16. Brix, J., Rüdiger, S., Bukau, B., Schneider-Mergener, J., and Pfanner, N. (1999) *J. Biol. Chem.* **274,** 16522–16530
17. Bolender, N., Sickmann, A., Wagner, R., Meisinger, C., and Pfanner, N. (2008) *EMBO Rep.* **9,** 42–49
18. Söllner, T., Pfaller, R., Griffiths, G., Pfanner, N., and Neupert, W. (1990) *Cell* **62,** 107–115
19. Tsuchimoto, D., Sakai, Y., Sakumi, K., Nishioka, K., Sasaki, M., Fujiwara, T., and Nakabeppu, Y. (2001) *Nucleic Acids Res.* **29,** 2349–2360
20. Jackson, E. B., Theriot, C. A., Chattopadhyay, R., Mitra, S., and Izumi, T. (2005) *Nucleic Acids Res.* **33,** 3303–3312
21. Dinur-Mills, M., Tal, M., and Pines, O. (2008) *PLoS ONE* **3,** e2161
22. Li, M. X., Wang, D., Zhong, Z. Y., Xiang, D. B., Li, Z. P., Xie, J. Y., Yang, Z. Z., Jin, F., and Qing, Y. (2008) *Free Radic. Biol. Med.* **45,** 592–601
23. Saeed, A. I., Sharov, V., White, J., Li, J., Liang, W., Bhagabati, N., Braisted, J., Klapa, M., Currier, T., Thiagarajan, M., Sturn, A., Snuffin, M., Rezantsev, A., Popov, D., Ryltsov, A., Kostukovich, E., Borisovsky, I., Liu, Z., Vinsavich, A., Trush, V., and Quackenbush, J. (2003) *BioTechniques* **34,** 374–378
24. Poot, M., Gibson, L. L., and Singer, V. L. (1997) *Cytometry* **27,** 358–364
25. Chacinska, A., Pfanner, N., and Meisinger, C. (2002) *Trends Cell Biol.* **12,** 299–303
26. Bhakat, K. K., Mantha, A. K., and Mitra, S. (2009) *Antioxid. Redox Signal.* **11,** 621–638
27. Vongsamphanh, R., Fortier, P. K., and Ramotar, D. (2001) *Mol. Cell. Biol.* **21,** 1647–1655
28. Otera, H., Taira, Y., Horie, C., Suzuki, Y., Suzuki, H., Setoguchi, K., Kato, H., Oka, T., and Mihara, K. (2007) *J. Cell Biol.* **179,** 1355–1363
29. Setoguchi, K., Otera, H., and Mihara, K. (2006) *EMBO J.* **25,** 5635–5647